*Desalination and Water Treatment*
www.deswater.com
doi: 10.5004/dwt.2017.21262

92 (2017) 1–8
October

# A simple method for the determination of adsorption kinetic parameters using circulating-type shallow bed reactor (CSBR)

Takashi Kawakita[a], Huan-Jung Fan[b,*], Yoshimi Seida[c], Tomohiro Kinoshita[d], Eiji Furuya[d]

[a]*Zenkosha Co. Ltd., Tokyo, Japan, email: takashi@zenko.co.jp*
[b]*Department of Safety, Health and Environmental Engineering, Hungkuang University, Taichung 433, Taiwan, Tel. +886 4 26318652; Fax: +886 4 26525245; email: fan@sunrise.hk.edu.tw*
[c]*Natural Science Laboratory, Toyo University, Tokyo, Japan, email: seida@toyo.jp*
[d]*Department of Applied Chemistry, Meiji University, Kawasaki, Japan, emails: tkino@meiji.ac.jp (T. Kinoshita); egfuruya@meiji.ac.jp (E. Furuya)*

Received 17 December 2016; Accepted 16 July 2017

**ABSTRACT**

This study focuses on a novel technique for determining intraparticle diffusivity ($D_p$) and fluid-film mass transfer coefficient ($k_F$) using a recycling type fixed-bed reactor. The detail analysis technique is established in this study. The $D_p$ and $k_F$ values of phenol on XAD-2000 are 7.26–11.4 × $10^{-6}$ ($cm^2$ $s^{-1}$) and 0.0035–0.0062 × $10^{-3}$ (cm $s^{-1}$), respectively. The obtained $D_p$ values are similar to the values obtained in the shallow bed reactor 1.6–2.7 × $10^{-6}$ ($cm^2$ $s^{-1}$). The method has significant advantages over the conventional shallow bed method in chemical/solution saving with easy operation. This technique is useful to estimate diffusivities of phenolic compounds onto resins, especially when the fluid-film mass transfer resistance cannot be negligible.

*Keywords:* Phenol; Recycling shallow bed reactor; Adsorption; Intraparticle diffusivity; Fluid film mass transfer coefficient

## 1. Introduction

Adsorptive separation processes are important for recovery or removal of chemicals in water or wastewater treatment [1–4]. To design an adsorptive separation process, both adsorption equilibrium and kinetic parameters are important [5]. In general, adsorption equilibrium parameters can be obtained from experiments easily. On the other hand, the determination of kinetic parameters such as intraparticle diffusivity ($D_p$) and fluid-film mass transfer coefficient ($k_F$) requires significant amount of efforts in both experimental and analytical works.

Commonly used experimental techniques for the determination of intraparticle diffusivities include long bed, shallow bed and completely mixed batch reactor (CMBR) [5]. In conventional analyses of batch reactor (such as CMBR) and shallow bed reactor, the fluid-film mass transfer resistance is neglected while determining the $D_p$ [6–9]. As a result, the accuracy of the obtained $D_p$ might be in question, if the fluid-film mass transfer resistance cannot be neglected. In the cases of resin particles, the fluid-film mass transfer resistance ($k_F$) of the resin beds cannot be neglected. Therefore, development of a simple and valid method for the estimation of the adsorption kinetics parameters of resin particle would be desired. In addition, intraparticle diffusion includes parallel pore and surface diffusion. In the case of adsorption by resins, the intraparticle diffusion is governed by pore diffusion [5,10,11].

In general, long bed and shallow bed techniques require significant amount of test solutions, while CMBR technique requires minimum amount of fluid volume [5,12]. This study combines advantages of both shallow bed and CMBR reactor. A novel determination technique is developed in this study to determine kinetic parameters ($D_p$ and $k_F$) using a circulating-type shallow bed reactor (CSBR). This method has the advantages of environmental-friendly, low cost and

* Corresponding author.

easy operation in comparison with conventional methods such as fixed-bed and shallow bed reactors.

## 2. Materials and methods

### 2.1. Adsorption isotherms

XAD-2000 and phenol (PHL) were employed as the adsorbent and adsorbate, respectively. Characteristics of the resin (XAD-2000) are listed in the Table 1. The resin was first prepared by being soaked and washed in isopropanol solution to remove impurities. The resulting resins were washed with distilled water to remove isopropanol. Then, the washed resins were soaked in 0.1 M NaOH aqueous solution to remove impurities. The impurities in the aqueous solution were monitored by UV–Vis to ensure proper cleaning. The resins were washed again with distilled water to remove NaOH and preserved with distilled water in a glass bottle until use.

Adsorption isotherms were determined using a conventional batch bottle technique at 293 K. In brief, a known amount of resin (about 0.1) (XAD-2000) was added into a series of 25 mL glass bottles that contained 20 mL of known concentrations of adsorbate (PHL). These bottles were mixed for 7 d (at 20°C). In previous work, Freundlich-type isotherm was well fitted for phenol resin systems [5,13]. Therefore, Freundlich isotherm was chosen in this study. The adsorption capacity ($q_e$, milligrams of adsorbate adsorbed/grams of absorbent) was determined using Eq. (1).

$$q = \left(\frac{V}{m}\right)(c_0 - c_e) \tag{1}$$

where $q$ is the adsorption capacity of resins (mg $g^{-1}$), $c_0$ and $c_e$ are initial and equilibrium concentrations of PHL (mg $L^{-1}$), respectively, $V$ is the solution volume and $m$ is the mass of adsorbent (g). The equilibrium concentration of the solution was measured by UV spectrophotometry (Shimadzu, UV1700, Japan) at a wavelength of 270.0 nm. Selected samples were analyzed in triplicate within accepted analytical error (±5%).

### 2.2. Kinetic studies

A new CSBR was proposed in this study. A typical experimental setup of the CSBR is shown in Fig. 1. A 1 L solution of known PHL concentration (about 1,000 mg/L) was prepared and added to a 2 L reservoir (vessel). The difference between the CSBR and a traditional shallow bed reactor is that the effluent of the shallow bed is redirected back to the reservoir as shown in Fig. 1. The reservoir was immersed in a constant temperature bath (298 K).

The liquid flow rate was set at 33.3 $cm^3\ s^{-1}$ (superficial linear velocity 1.41 cm $s^{-1}$). Detailed experimental conditions are listed in Table 2. The aliquot amounts of solution (1 mL) were periodically sampled to determine the PHL concentrations. Selected samples were analyzed in triplicate within accepted analytical error (±5%).

Table 1
Characteristics of XAD-2000

| Resin | XAD-2000 |
|---|---|
| Particle size (mm) | 0.194 |
| Pore volume (mL $g^{-1}$) | 0.73 |
| Mean pore diameter (Å) | 45 |
| $\rho_s$ (g $mL^{-1}$) | 0.650 |
| Specific surface area ($m^2\ kg^{-1}$)[a] | 0.62 |

[a]Provided by Organo Corporation, Japan with mercury intrusion methods.

## 3. Results and discussion

### 3.1. Mathematical model

The fundamental equations of the reactor are listed in Eqs. (2)–(6). These equations are based on the following

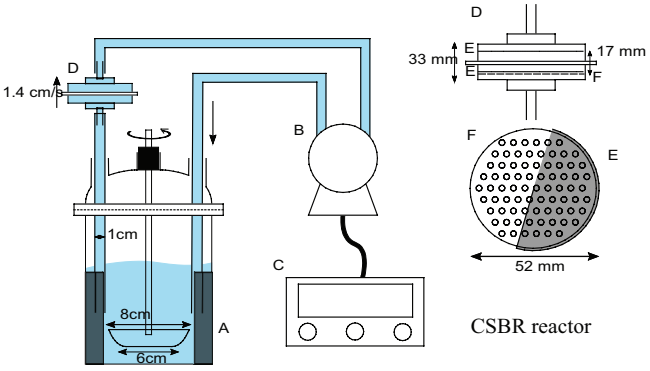


Fig. 1. Experimental setup of circulating-type shallow bed reactor (CSBR) (A, baffle plate; B, peristaltic pump drive; C, digital modular drive; D, column; E, stainless mesh; F, dispersion plate).

Table 2
Typical experimental conditions

| Parameters | Value |
|---|---|
| Freundlich, $k$ | 1.84 |
| Freundlich, $n$ | 1.75 |
| Initial concentration $C_0$ (mg $L^{-1}$) | 1,000.6 |
| Fluid volume ($cm^3$) | 1,000 |
| Sectional area of shallow bed ($cm^2$) | 23.7 |
| Whole shallow bed volume ($cm^3$) | 35.6 |
| Shallow bed volume ($cm^3$) | 23.7 |
| Shallow bed height (cm) | 1 |
| Shallow bed volume (g $cm^{-3}$) | 0.35 |
| Shallow bed void fraction | 0.33 |
| Volumetric flow rate ($cm^3\ s^{-1}$) | 33.3 |
| Linear flow rate (cm $s^{-1}$) | 1.41 |
| Packed shallow bed resin particle volume (g) | 8.2 |
| Apparent solid density (g $L^{-1}$) | 602.8 |
| Resin particle diameter (cm) | 0.0356 |
| Resin particle volume ($cm^3$) | 0.001327 |

assumptions of (1) spherical particle geometry of resin, (2) a constant flow rate, (3) constant temperature, (4) pore diffusion control, (5) the establishment of a local equilibrium at the fluid-to-solid interface and (6) a Freundlich-type isotherm. Axial dispersion was neglected in this study.

Mass balance within the bed:

$$u\left(\frac{\partial c_t}{\partial z}\right)+\varepsilon_B\left(\frac{\partial c_t}{\partial t}\right)+\rho_B\left(\frac{\partial q_t}{\partial t}\right)=0 \tag{2}$$

Mass balance within particles:

$$\rho_S\left(\frac{\partial q_m}{\partial t}\right)=\left(\frac{D_p}{r^2}\right)\frac{\partial}{\partial r}\left(r^2\frac{\partial c_m}{\partial r}\right) \tag{3}$$

Mass transfer within fluid film:

$$\rho_B\left(\frac{\partial q_t}{\partial t}\right)=k_F a_V(c_t-c_S) \tag{4}$$

Mass transfer on geometric surface:

$$\rho_B\left(\frac{\partial q_t}{\partial t}\right)=-D_p\,a_V\left(\frac{\partial c_m}{\partial r}\right)_{r=r_p} \tag{5}$$

Mass balance within vessel:

$$\left(\frac{\partial c_{t,in}}{\partial t}\right)=\left(\frac{Au}{V}\right)(c_{t,out}-c_{t,in}) \tag{6}$$

To reduce the number of variables, eight dimensionless variables (Eqs. (7)–(15)) were introduced for converting these equations into dimensionless equations (Eqs. (16)–(20)). These dimensionless variables could minimize the number of parameters and reduce the amount of numerical calculation of these equations.

Dimensionless variables:

$$T=\left(\frac{1}{\beta\rho_S}\right)\left(\frac{D_P}{r_P^2}\right)t \qquad \left(\frac{\partial T}{\partial t}\right)=\left(\frac{1}{\beta\rho_S}\right)\left(\frac{D_P}{r_P^2}\right) \tag{7}$$

$$Z=\left(\frac{D_P}{r_P^2}\right)\left(\frac{\rho_B}{\rho_S}\right)\left(\frac{z}{u}\right) \qquad \left(\frac{\partial Z}{\partial z}\right)=\left(\frac{D_P}{r_P^2}\right)\left(\frac{\rho_B}{\rho_S}\right)\left(\frac{1}{u}\right) \tag{8}$$

$$R=\frac{r}{r_P} \qquad \frac{\partial R}{\partial r}=\frac{1}{r_P} \tag{9}$$

$$C=\frac{c}{c_0} \qquad \frac{\partial c}{\partial C}=c_0 \tag{10}$$

$$Q=\frac{q}{q_0} \qquad \frac{\partial q}{\partial Q}=q_0 \tag{11}$$

$$\alpha=\frac{\varepsilon_B}{\beta\rho_B} \tag{12}$$

$$Bi=\frac{k_F r_P}{D_P} \tag{13}$$

$$\phi=\left(\frac{Aur_P^2\beta\rho_S}{V\,D_P}\right) \tag{14}$$

$$\phi Z=\left(\frac{Aur_P^2\beta\,\rho_S}{V\,D_P}\right)\left(\frac{D_P}{r_P^2}\right)\left(\frac{\rho_B}{\rho_S}\right)\left(\frac{z}{u}\right)=\left(\frac{Az\rho_B\beta}{V}\right) \tag{15}$$

Fundamental dimensionless equations

Mass balance within the bed:

$$\frac{\partial C_t}{\partial Z}+\alpha\frac{\partial C_t}{\partial T}+\frac{\partial Q_t}{\partial T}=0 \qquad \alpha=\frac{\varepsilon_B}{\beta\rho_B} \tag{16}$$

Mass balance within particles:

$$\left(\frac{\partial Q_m}{\partial T}\right)=\left(\frac{1}{R^2}\right)\frac{\partial}{\partial R}\left(R^2\frac{\partial C_m}{\partial R}\right) \tag{17}$$

Mass transfer within fluid film:

$$\left(\frac{\partial Q_t}{\partial T}\right)=3Bi(C_t-C_S) \qquad Bi=\frac{k_F r_P}{D_P} \tag{18}$$

Mass transfer on geometric surface:

$$\left(\frac{\partial Q_t}{\partial T}\right)=-3\left(\frac{\partial C_m}{\partial R}\right)_{R=1} \tag{19}$$

Mass balance within vessel:

$$\left(\frac{\partial C_{t,in}}{\partial T}\right)=\phi(C_{t,out}-C_{t,in}) \qquad \phi=\left(\frac{Aur_P^2\beta\rho_S}{V\,D_P}\right) \tag{20}$$

The above dimensionless fundamental equations (Eqs. (16)–(20)) were solved numerically to obtain theoretical concentration decay curves for the CSBR. The obtained theoretical concentration decay curves were used for determination of $D_p$ and $k_F$.

The implicit method was employed to solve the finite difference equations. Computation software for these calculations was written with the Borland C++ Builder.

Note that the value of $\phi Z$ was exactly the same as the solid-to-liquid ratio employed in the CMBR. This means that the technique used in CMBR concentration decay curves can be estimated from experimental conditions for the CSBR as well.

The detail derivation of fundamental equations into dimensionless fundamental equations is given in Appendix A.

### 3.2. Determination of adsorption isotherm

The adsorption isotherm of PHL onto the resin was determined and is shown in Fig. 2. The Freundlich isotherm is listed in Eq. (21) and Freundlich constants, $k$ and $n$, were obtained as 1.84 and 1.75, respectively.

$$q = 1.84 \times C_e^{1/1.75} \quad (21)$$

### 3.3. Determination of experimental dimensional and dimensionless concentration decay curves

Five sets of kinetic experiments (experimental runs a–e) were performed with the CSBR systems. The experimental conditions and results are presented in Table 3 and Fig. 3, respectively.

The experimental dimensional concentration decay curves (Fig. 3) were converted into dimensionless concentration decay curves as shown in Fig. 4. As shown, all these curves were converted into one curve. This result was similar to the findings reported by Sonetaka et al. [10]. They investigated PHL adsorbed onto granular activated carbon in a shallow bed reactor.

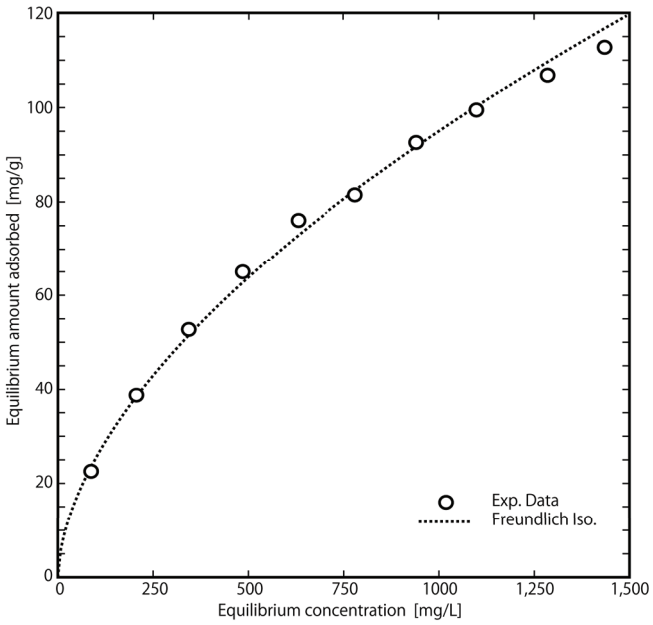


Fig. 2. Freundlich isotherm of PHL onto XAD-2000.

### 3.4. Determination of $t_{0.3}/t_{07}$ and $T_{0.3}/T_{0.7}$

The ratios of $t_{0.3}/t_{07}$ or $T_{0.3}/T_{07}$ could be determined from experimental dimensionless decay curves (Fig. 5). $T_{0.3}/T_{07}$ was equal to $t_{0.3}/t_{07}$ as demonstrated in the following equation:

$$\frac{T_{0.3}}{T_{0.7}} = \frac{\left(\frac{D_P}{r_P^2 \beta \rho_S}\right) t_{0.3}}{\left(\frac{D_P}{r_P^2 \beta \rho_S}\right) t_{0.7}} = \frac{t_{0.3}}{t_{0.7}} \quad (22)$$

Dimensional time $t_{0.3}$ and $t_{0.7}$ was corresponding to the dimensionless concentrations at 0.3 and 0.7, respectively, as shown in the Fig. 5. Using experimental run "a" data as an example, $t_{03}$ and $t_{0.7}$ were equal to 3.51 and 0.708, respectively (Fig. 5). As a result, $t_{0.3}/t_{07} = T_{0.3}/T_{07} = 4.96$ as shown in Table 3.

### 3.5. Determination of T/t

The ratio of $T/t$ can be determined by matching theoretical and experimental decay curves. Using experimental run "a" as an example, the theoretical and experimental decay curves were overlaid by shifting one of the curves horizontally until the two curves matched as shown in Fig. 6. As indicated in the figure, $T/t$ was equal to 0.019 ($min^{-1}$) obtained by curve matching (e.g., $T = 0.019$, $t = 10° = 1$ $min^{-1}$, then $T/t = 0.019$ $min^{-1}$).

### 3.6. Determination of $D_p$

The $T/t$ is substituted into Eq. (7) to evaluate the intraparticle diffusivity, $D_p$.

$$D_p = \left(\frac{T}{t}\right)(r_P^2 \beta \rho_S) \quad (23)$$

Table 3
Experimental conditions and results

| Experimental runs | a | b | c | d | e |
|---|---|---|---|---|---|
| Resin (wet, g) | 15.21 | 8.21 | 16.02 | 16.05 | 16.03 |
| Resin (dry, g) | 7.25 | 3.92 | 7.64 | 7.65 | 7.64 |
| Freundlich, $k$ | 1.84 | 1.84 | 1.84 | 1.84 | 1.84 |
| Freundlich, $n$ | 1.75 | 1.75 | 1.75 | 1.75 | 1.75 |
| $C_e$ (mg $L^{-1}$) | 553 | 711 | 590 | 604 | 591 |
| $t_{0.3}/t_{0.7}$ | 4.96 | 5.11 | 5.15 | 5.33 | 5.01 |
| $B_i$ | 10.10 | 10.20 | 10.30 | 11.60 | 9.30 |
| $T/t$ ($min^{-1}$) | 1.90E-02 | 1.60E-02 | 2.50E-02 | 2.50E-02 | 2.20E-02 |
| $r_p$ (cm) | 0.021 | 0.021 | 0.021 | 0.021 | 0.021 |
| $\beta$ (L $g^{-1}$) | 9.43E-02 | 9.50E-02 | 9.53E-02 | 9.46E-02 | 9.47E-02 |
| $\rho_s$ (g $L^{-1}$) | 650 | 650 | 650 | 650 | 650 |
| $D_p$ ($cm^2$ $s^{-1}$) | 8.6E-06 | 7.3E-06 | 1.1E-05 | 1.1E-05 | 9.9E-06 |
| $k_F$ (cm $s^{-1}$) | 4.1E-03 | 3.5E-03 | 5.6E-03 | 6.2E-03 | 4.5E-03 |

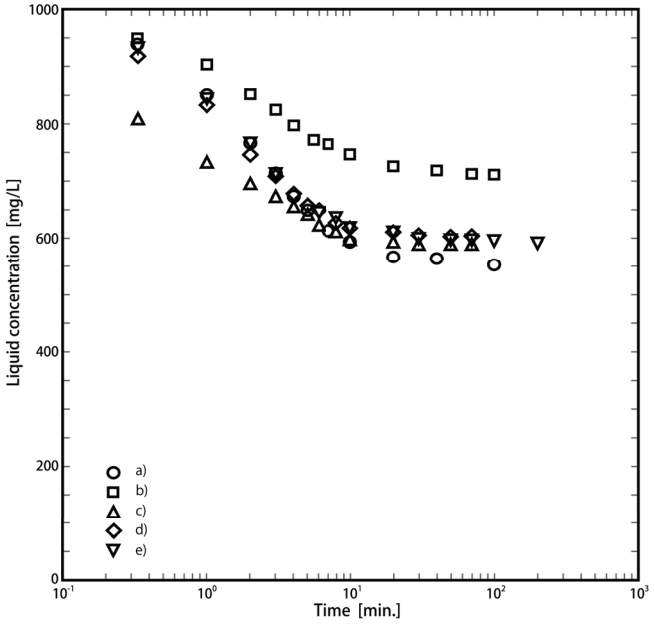


Fig. 3. Experimental dimensional concentration decay curves of PHL onto XAD-2000. Symbols (a–e) are corresponding to the experimental runs (a–e) listed in Table 3.

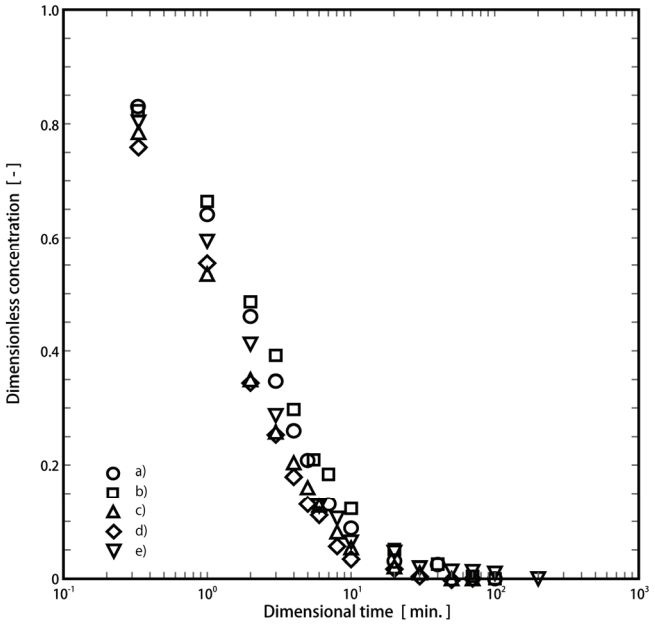


Fig. 4. Experimental dimensionless concentration decay curves (EDCDC) of PHL onto XAD-2000. Symbols (a–e) are corresponding to the experimental runs (a–e) listed in Table 3.

The obtained $D_p$ is listed in Table 3 (7.26–11.38 × $10^{-6}$ ($cm^2$ $s^{-1}$). This result was similar to the values obtained in the shallow bed reactor 1.6–2.7 × $10^{-6}$ ($cm^2$ $s^{-1}$) (in this study) and in the CMBR method [5] (11 × $10^{-6}$ $cm^2$ $s^{-1}$, XAD-2000, PHL). However, this result was slightly higher than the values reported by Satoh et al. [8] (8.00 × $10^{-8}$ $cm^2$ $s^{-1}$, resin, PHL, shallow bed method), (1.42–3.22 × $10^{-8}$ $cm^2$ $s^{-1}$, activated carbon, phenol, shallow bed method, [14]) and (6.3 × $10^{-8}$ $cm^2$ $s^{-1}$, activated carbon, phenol, shallow bed method, [10]).

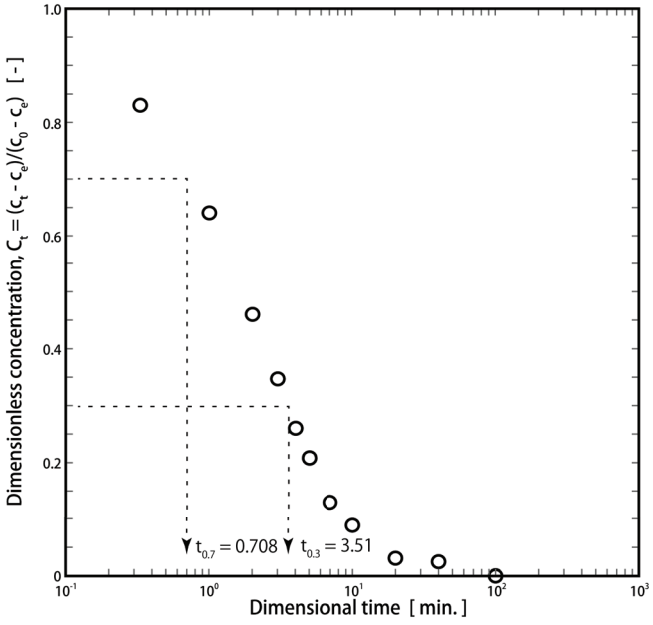


Fig. 5. Correlations between $T$ ($T_{0.3}$ and $T_{0.7}$) and dimensionless concentrations (experimental run a).

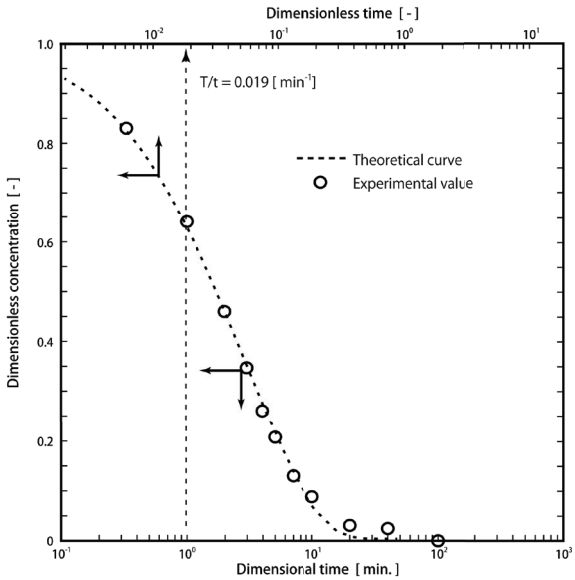


Fig. 6. Matching plot of experimental and theoretical dimensionless concentration decay curves (experimental run a).

### 3.7. Determination of $B_i$

The relationship between Biot number and $T_{0.3}/T_{0.7}$ as shown in Fig. 7 could be used for determining $B_i$ with known ratios of $T_{0.3}/T_{0.7}$. In general, the values of $B_i$ have significant impact on the mass transfer of adsorbates. For example, the adsorption rates controlled by (1) fluid-film mass transfer, (2) intraparticle diffusion and the fluid-film mass transfer and (3) intraparticle diffusion were $B_i < 1$, $1 < B_i < 300$ and $B_i > 300$ regions, respectively [10]. For example, $B_i$ obtained in this study was in the ranges of 4.96–5.33 (Table 3). This result was in agreement with previous assumptions that both intraparticle diffusion and the fluid-film mass transfer were important in the XAD-2000 PHL system.

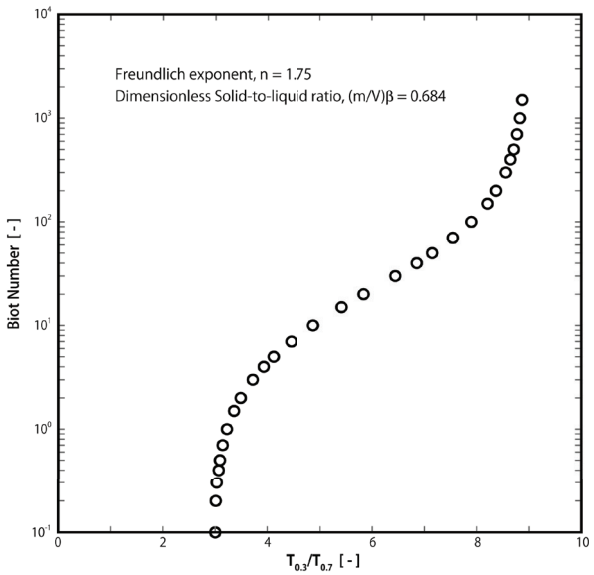


Fig. 7. Relationship between Biot number and $T_{0.3}/T_{0.7}$ (experimental run a).

### 3.8. Determination of $k_F$

The fluid-film mass transfer coefficient ($k_F$) can be determined in Eq. (13). Intraparticle diffusivity ($D_p$) and Biot number ($B_i$) evaluated in previous sections are substituted to Eq. (13).

$$k_F = B_i \times D_p / r_p \quad (24)$$

The obtained $k_F$ was about 0.0035–0.0062 × $10^{-3}$ (cm $s^{-1}$) as shown in Table 3.

$B_i$ (4.96 to 5.33) obtained in this study indicated that both intraparticle diffusion and the fluid-film mass transfer were important in resins-PHL system. Therefore, conventional analyses of batch reactor (such as CMBR) and shallow bed reactor could not apply in this case, since these methods neglected the fluid-film mass transfer resistance while determining the $D_p$. Therefore, the method (CSBR) developed in this study is useful to estimate diffusivities of phenolic compounds onto resins, especially when the fluid-film mass transfer resistance cannot be negligible.

## 4. Conclusions

A novel technique for determining $D_p$ and $k_F$ using the CSBR is presented in this study. The obtained $D_p$ and $k_F$ values of phenol on XAD-2000 are 7.26–11.38 × $10^{-6}$ ($cm^2$ $s^{-1}$) and 0.0035–0.0062 × $10^{-3}$ (cm $s^{-1}$), respectively. The results are more accurate than those obtained by the conventional technique. The proposed technique will be useful for estimating $D_p$ and $k_F$ of adsorption systems when both fluid-film mass transport and intraparticle diffusion resistance are significant.

## Symbols

| | | |
|---|---|---|
| $A$ | — | Column cross-sectional area |
| $a_v$ | — | Particle surface area per unit volume of bed |
| $a_P$ | — | Particle surface area per unit volume of adsorbent particle |
| $c_0$ | — | Influent solution concentration at $t = 0$ |
| $c_S$ | — | Fluid concentration at $r = r_p$ |
| $c_t$ | — | Fluid concentration at $t = t$ and $z = z$ |
| $c_{t,\text{in}}$ | — | Influent solution concentration at $t = t$ |
| $c_{t,\text{out}}$ | — | Effluent solution concentration at $t = t$ |
| $k_F$ | — | Fluid-film mass transfer coefficient |
| $n$ | — | Freundlich coefficient |
| $q_0$ | — | Equilibrium amount adsorbed with fluid concentration $c_0$ |
| $q_m$ | — | Amount adsorbed at $r = r$ |
| $q_S$ | — | Amount adsorbed at $r = r_p$ |
| $r_p$ | — | Particle radius |
| $u$ | — | Linear velocity |
| $V$ | — | Solution volume in tank |
| $z$ | — | Bed height |
| $\beta$ | — | Slope of operational line, $q_0/c_0$ |
| $\varepsilon_B$ | — | Bed void fraction |
| $\rho_B$ | — | Apparent bed density |

## References

[1] C. Tien, Adsorption Calculations and Modeling, Butterworth-Heinemann, Boston, USA, 1994.
[2] H.J. Fan, P.R. Anderson, Copper and cadmium removal by Mn oxide-coated granular activated carbon, Sep. Purif. Technol., 45 (2005) 61–67.
[3] L.A. Al-Khateeb, S. Almotiry, M. Abdel Salam, Adsorption of pharmaceutical pollutants onto graphene nanoplatelets, Chem. Eng. J., 248 (2014) 191–199.
[4] T. Kinoshita, H.J. Fan, T. Kawakita, E. Furuya, Optimization of a modification technique for reducing irreversible adsorption within synthetic resins, Adsorpt. Sci. Technol., 34 (6) (2016) 345–354.
[5] T. Kawakita, H.J. Fan, Y. Seida, J. Fujiki, E. Furuya, A simplified technique to determine intraparticle diffusivity of macroreticular resins, Sustain. Environ. Res., 26 (2016) 249–254.
[6] M. Suzuki, K. Kawazoe, Batch measurement of adsorption rate in an agitated tank–pore diffusion kinetics with irreversible isotherms, J. Chem. Eng. Jpn., 7 (1974) 346–350.
[7] D.W. Hand, J.C. Crittenden, M. ASCE, W.E. Thacker, User-orientated batch reactor solutions to the homogeneous surface diffusion model, J. Environ. Eng., 109 (1983) 82–101.
[8] K. Satoh, H.J. Fan, H. Hattori, K. Tajima, E. Furuya, Simultaneous determination of intraparticle diffusivities from ternary component uptake curves using the shallow bed technique, J. Hazard. Mater., 155 (2008) 397–402.
[9] E.G. Furuya, H.T. Chang, Y. Miura, H. Yokoyama, S. Tajima, S. Yamashita, K.E. Noll, Intraparticle mass transport mechanism in activated carbon adsorption of phenols, J. Environ. Eng., 122 (1996) 909–916.
[10] N. Sonetaka, H.J. Fan, S. Kobayashi, H.N. Chang, E. Furuya, Simultaneous determination of intraparticle diffusivity and liquid film mass transfer coefficient from a single-component adsorption uptake curve, J. Hazard. Mater., 164 (2009) 1447–1451.
[11] J. Fujiki, K. E. Noll, T. Kawakita, Y. Nakane, E. Furuya, Simplified determination method of intraparticle diffusivity within a resin adsorbent from binary-component liquid adsorption uptake curves, Transp. Porous Media, 102 (2014) 349–364.
[12] J. Fujiki, N. Sonetaka, K.P. Ko, E. Furuya, Experimental determination of intraparticle diffusivity and fluid film mass transfer coefficient using batch contactors, Chem. Eng. J., 160 (2010) 683–690.
[13] J. Fujiki, T. Shinomiya, T. Kawakita, S. Ishibashi, E. Furuya, Experimental determination of fluid-film mass transfer coefficient from adsorption uptake curve, Chem. Eng. J., 173 (2011) 49–54.
[14] T. Kinoshita, H. J. Fan, E. Furuya, An innovative method for determining micro pore volume of synthetic resins, Colloids Surf., A, 466 (2015) 107–114.

# Appendix A

Mass balance within the bed:

$$u\left(\frac{\partial c_t}{\partial z}\right)+\varepsilon_B\left(\frac{\partial c_t}{\partial t}\right)+\rho_B\left(\frac{\partial q_t}{\partial t}\right)=0 \tag{1}$$

$$u\left\{\left(\frac{\partial c_t}{\partial C_t}\right)\left(\frac{\partial Z}{\partial z}\right)\left(\frac{\partial C_t}{\partial Z}\right)\right\}+\varepsilon_B\left\{\left(\frac{\partial c_t}{\partial C_t}\right)\left(\frac{\partial T}{\partial t}\right)\left(\frac{\partial C_t}{\partial T}\right)\right\}+\rho_B\left\{\left(\frac{\partial q_t}{\partial Q_t}\right)\left(\frac{\partial T}{\partial t}\right)\left(\frac{\partial Q_t}{\partial T}\right)\right\}=0$$

$$u\left\{(c_0)\left(\frac{D_P}{r_P^2}\right)\left(\frac{\rho_B}{\rho_S}\right)\left(\frac{1}{u}\right)\left(\frac{\partial C_t}{\partial Z}\right)\right\}+\varepsilon_B\left\{(c_0)\left(\frac{1}{\beta\rho_S}\right)\left(\frac{D_P}{r_P^2}\right)\left(\frac{\partial C_t}{\partial T}\right)\right\}+\rho_B\left\{(q_0)\left(\frac{1}{\beta\rho_S}\right)\left(\frac{D_P}{r_P^2}\right)\left(\frac{\partial Q_t}{\partial T}\right)\right\}=0$$

$$u\left\{\left(\frac{\rho_B}{\rho_S}\right)\left(\frac{1}{u}\right)\left(\frac{\partial C_t}{\partial Z}\right)\right\}+\varepsilon_B\left\{\left(\frac{1}{\beta\rho_S}\right)\left(\frac{\partial C_t}{\partial T}\right)\right\}+\rho_B\left\{\left(\frac{q_0}{c_0}\right)\left(\frac{1}{\beta\rho_S}\right)\left(\frac{\partial Q_t}{\partial T}\right)\right\}=0$$

$$\left(\frac{\rho_B}{\rho_S}\right)\left(\frac{\partial C_t}{\partial Z}\right)+\left(\frac{\varepsilon_B}{\beta\rho_S}\right)\left(\frac{\partial C_t}{\partial T}\right)+\left(\frac{\beta\rho_B}{\beta\rho_S}\right)\left(\frac{\partial Q_t}{\partial T}\right)=0$$

$$\left(\frac{\rho_B}{\rho_S}\right)\left(\frac{\partial C_t}{\partial Z}\right)+\left(\frac{\varepsilon_B}{\beta\rho_S}\right)\left(\frac{\partial C_t}{\partial T}\right)+\left(\frac{\rho_B}{\rho_S}\right)\left(\frac{\partial Q_t}{\partial T}\right)=0$$

$$\left(\frac{\partial C_t}{\partial Z}\right)+\left(\frac{\varepsilon_B}{\beta\rho_B}\right)\left(\frac{\partial C_t}{\partial T}\right)+\left(\frac{\partial Q_t}{\partial T}\right)=0 \quad \alpha=\left(\frac{\varepsilon_B}{\beta\rho_B}\right)$$

$$\left(\frac{\partial C_t}{\partial Z}\right)+\alpha\left(\frac{\partial C_t}{\partial T}\right)+\left(\frac{\partial Q_t}{\partial T}\right)=0 \tag{15}$$

Mass balance within particles:

$$\rho_S\left(\frac{\partial q_m}{\partial t}\right)=\left(\frac{D_P}{r^2}\right)\frac{\partial}{\partial r}\left(r^2\frac{\partial c_m}{\partial r}\right)$$

$$\rho_S\left(\frac{\partial q_m}{\partial Q_m}\frac{\partial T}{\partial t}\frac{\partial Q_m}{\partial T}\right)=\left(\frac{D_p}{r^2}\right)\frac{\partial}{\partial R}\frac{\partial R}{\partial r}\left(r^2\frac{\partial c_m}{\partial C_m}\frac{\partial R}{\partial r}\frac{\partial C_m}{\partial R}\right) \tag{2}$$

$$\rho_S\left(q_0\frac{D_P}{r_P^2\beta\,\rho_S}\frac{\partial Q_m}{\partial T}\right)=\left(\frac{D_P}{R^2r_P^2}\right)\frac{\partial}{\partial R}\frac{1}{r_P}\left(R^2r_P^2c_0\frac{1}{r_P}\frac{\partial C_m}{\partial R}\right)$$

$$\rho_S\left(q_0\frac{D_P}{r_P^2\beta\,\rho_S}\frac{\partial Q_m}{\partial T}\right)=\left(c_0\frac{D_P}{r_P^2}\frac{1}{R^2}\right)\frac{\partial}{\partial R}\left(R^2\frac{\partial C_m}{\partial R}\right)$$

$$\left(\frac{\rho_S}{\rho_S}\right)\left(\frac{q_0}{c_0}\right)\left(\frac{1}{\beta}\right)\left(\frac{\partial Q_m}{\partial T}\right)=\left(\frac{1}{R^2}\right)\frac{\partial}{\partial R}\left(R^2\frac{\partial C_m}{\partial R}\right)$$

$$(\beta)\left(\frac{1}{\beta}\right)\left(\frac{\partial Q_m}{\partial T}\right)=\left(\frac{1}{R^2}\right)\frac{\partial}{\partial R}\left(R^2\frac{\partial C_m}{\partial R}\right) \tag{16}$$

$$\left(\frac{\partial Q_m}{\partial T}\right)=\left(\frac{1}{R^2}\right)\frac{\partial}{\partial R}\left(R^2\frac{\partial C_m}{\partial R}\right)$$

Mass transfer within fluid film:

$$\rho_B\left(\frac{\partial q_t}{\partial t}\right)=k_Fa_V\left(c_t-c_S\right)$$

$$\rho_B\left(\frac{\partial q_t}{\partial Q_t}\frac{\partial T}{\partial t}\frac{\partial Q_t}{\partial T}\right)=k_Fa_Vc_0\left(C_t-C_S\right)$$

$$\rho_B\left(q_0\frac{D_P}{r_P^2\beta\,\rho_S}\frac{\partial Q_t}{\partial T}\right)=k_Fa_Vc_0\left(C_t-C_S\right) \tag{3}$$

$$\left(\frac{\partial Q_t}{\partial T}\right)=k_Fa_Vc_0\frac{r_P^2}{D_P\,c_0}\frac{\rho_S}{\rho_B}\left(C_t-C_S\right)$$

$$\left(\frac{\partial Q_t}{\partial T}\right)=\frac{k_Fa_Vr_P^2}{D_P}\frac{\rho_S}{\rho_B}\left(C_t-C_S\right)$$

Derivation of $\rho_S/\rho_B$:

Volume of one particle $v=\frac{4}{3}\pi r_P^3$

Weight of one particle $w=\frac{4}{3}\pi r_P^3\rho_S$

Total weight of solids within bed volume $V$ $W=V\,\rho_B$

Number of solids within bed volume $V$ $n=\frac{W}{w}$

Total solid volume within bed volume $V$

$$n\,v=n\frac{4}{3}\pi r_P^3=\frac{W}{\frac{4}{3}\pi r_P^3\rho_S}\frac{4}{3}\pi r_P^3=\frac{W}{\rho_S}$$

Bed void fraction

$$\varepsilon_B=\frac{V-(nv)}{V}=1-\frac{(nv)}{V}=1-\frac{W}{V\rho_S}=1-\frac{\rho_B}{\rho_S}$$

Then, $\frac{\rho_S}{\rho_B} = \frac{1}{1-\varepsilon_B}$

Derivation of $a_V$:

Volume of one particle $v = \frac{4}{3}\pi r_P^3$

Weight of one particle $w = \frac{4}{3}\pi r_P^3 \rho_S$

Geometric surface area of one particle $s = 4\pi r_P^2$

Number of solids within bed volume $V$

$$n = \frac{V\rho_B}{w} = \frac{V\ \rho_B}{\frac{4}{3}\pi r_P^3 \rho_S}$$

Then, $a_V = \frac{sn}{V} = \frac{4\pi r_P^2}{V}\frac{V\ \rho_B}{\frac{4}{3}\pi r_P^3 \rho_S} = \frac{3}{r_P}\frac{\rho_B}{\rho_S}$

$$\left(\frac{\partial Q_t}{\partial T}\right) = \frac{k_F r_P^2}{D_P}\frac{3}{r_P}\frac{\rho_B}{\rho_S}\frac{\rho_S}{\rho_B}\left(C_t - C_S\right)$$
$$\left(\frac{\partial Q_t}{\partial T}\right) = 3\frac{k_F r_P}{D_P}\left(C_t - C_S\right) \quad (17)$$
$$\left(\frac{\partial Q_t}{\partial T}\right) = 3Bi\left(C_t - C_S\right)$$

where $Bi = \frac{k_F r_P}{D_P}$.

Mass transfer at geometric surface:

$$\rho_S\left(\frac{\partial q_t}{\partial t}\right) = -D_P a_P\left(\frac{\partial c_m}{\partial r}\right)_{r=r_P}$$
$$\rho_S\left(\frac{\partial q_t}{\partial Q_t}\frac{\partial T}{\partial t}\frac{\partial Q_t}{\partial T}\right) = -D_P a_P\left(\frac{\partial c_m}{\partial C_m}\frac{\partial R}{\partial r}\frac{\partial C_m}{\partial R}\right)_{R=1} \quad (4)$$

Derivation of $a_V$:

Volume of one particle $v = \frac{4}{3}\pi r_P^3$

Geometric surface area of one particle $s = 4\pi r_P^2$

Then, $a_P = \frac{s}{v} = \frac{4\pi r_P^2}{\frac{4}{3}\pi r_P^3} = \frac{3}{r_P}$

$$\rho_S\left(q_0\frac{D_P}{r_P^2\beta\rho_S}\frac{\partial Q_t}{\partial T}\right) = -D_P\frac{3}{r_P}\left(c_0\frac{1}{r_P}\frac{\partial C_m}{\partial R}\right)_{R=1}$$
$$\left(\frac{\partial Q_t}{\partial T}\right) = -3\left(\frac{\partial C_m}{\partial R}\right)_{R=1} \quad (18)$$

$$\left(\frac{\partial c_{t,\text{in}}}{\partial t}\right) = \left(\frac{Au}{V}\right)\left(c_{t,\text{out}} - c_{t,\text{in}}\right)$$
$$\left(\frac{\partial c_{t,\text{in}}}{\partial C_{t,\text{in}}}\frac{\partial T}{\partial t}\frac{\partial C_{t,\text{in}}}{\partial T}\right) = \left(\frac{Au}{V}\right)c_0\left(C_{t,\text{out}} - C_{t,\text{in}}\right)$$
$$\left(c_0\frac{D_P}{r_P^2\beta\rho_S}\frac{\partial C_{t,\text{in}}}{\partial T}\right) = \left(\frac{Au}{V}\right)c_0\left(C_{t,\text{out}} - C_{t,\text{in}}\right) \quad (5)$$
$$\left(\frac{\partial C_{t,\text{in}}}{\partial T}\right) = \left(\frac{Au r_P^2\beta\rho_S}{V D_P}\right)\left(C_{t,\text{out}} - C_{t,\text{in}}\right)$$

$$\left(\frac{\partial C_{t,\text{in}}}{\partial T}\right) = \phi\left(C_{t,\text{out}} - C_{t,\text{in}}\right) \quad (19)$$

where $\phi = \left(\frac{Au r_P^2\beta\rho_S}{V D_P}\right)$